ORIGINAL RESEARCH

Design of acid-responsive polymeric nanoparticles for 7,3′,4′-trihydroxyisoflavone topical administration

Pao-Hsien Huang,[1,*] Stephen Chu-Sung Hu,[2,3,*] Chiang-Wen Lee,[4,5] An-Chi Yeh,[6] Chih-Hua Tseng,[7] Feng-Lin Yen[1,8,9]

[1]Department of Fragrance and Cosmetic Science, College of Pharmacy, Kaohsiung Medical University, Kaohsiung, [2]Department of Dermatology, College of Medicine, Kaohsiung Medical University, Kaohsiung, [3]Department of Dermatology, Kaohsiung Medical University Hospital, Kaohsiung, [4]Research Center for Industry of Human Ecology, Chang Gung University of Science and Technology, Kweishan, Taoyuan, [5]Department of Nursing, Division of Basic Medical Sciences, Chang Gung University of Science and Technology, Chia-Yi, [6]Department of Cosmetics and Fashion Styling, Cheng Shiu University, Kaohsiung, [7]School of Pharmacy, College of Pharmacy, Kaohsiung Medical University, Kaohsiung, [8]Lipid Science and Aging Research Center, Kaohsiung Medical University, Kaohsiung, [9]Institute of Biomedical Sciences, National Sun Yat-Sen University, Kaohsiung, Taiwan

*These authors contributed equally to this work

Correspondence: Chih-Hua Tseng
School of Pharmacy, College of Pharmacy, Kaohsiung Medical University, 100 Shih-Chuan 1st Road, Kaohsiung 807, Taiwan
Tel +886 7 312 1101 ext 2163
Fax +886 7 321 0683
Email chihhua@kmu.edu.tw

Feng-Lin Yen
Department of Fragrance and Cosmetic Science, College of Pharmacy, Kaohsiung Medical University, 100 Shih-Chuan 1st Road, Kaohsiung 807, Taiwan
Tel +886 7 312 1101 ext 2028
Fax +886 7 321 0683
Email flyen@kmu.edu.tw

Abstract: 7,3′,4′-Trihydroxyisoflavone (734THIF) is a secondary metabolite of daidzein and has been recently found to possess antioxidant, melanin inhibition, and skin cancer chemopreventive activities. However, the poor water solubility of 734THIF impedes its absorption and skin penetration and, therefore, limits its pharmacological effects when applied topically to the skin. We seek to use the nanoprecipitation method to prepare optimal eudragit E100 (EE)–polyvinyl alcohol (PVA)-loaded 734THIF nanoparticles (734N) to improve its physicochemical properties and thereby increase its water solubility, skin penetration, and biological activities. EE–PVA-loaded 734THIF nanoparticles (734N) were prepared, and their morphology and particle size were evaluated using a particle size analyzer and by electron microscopy. The drug loading and encapsulation efficiencies and in vitro solubility were determined using high-performance liquid chromatography. Hydrogen-bond formation was evaluated by [1]H-nuclear magnetic resonance and Fourier transform infrared spectroscopy, and crystalline-to-amorphous transformation was determined by differential scanning calorimetry and X-ray diffractometry. In vitro skin penetration was analyzed using fresh pig skin mounted on Franz diffusion cells, and cytotoxicity against human keratinocyte HaCaT cells was evaluated using the MTT assay. Antioxidant activity was determined by 2,2-diphenyl-1-picrylhydrazyl-free radical scavenging ability. EE–PVA-loaded 734THIF nanoparticles showed good drug loading and encapsulation efficiencies and were characterized by improved physicochemical properties, including reduction in particle size, amorphous transformation, and intermolecular hydrogen-bond formation. This is associated with increased water solubility and enhanced in vitro skin penetration, with no cytotoxicity toward HaCaT cells. In addition, 734THIF nanoparticles retained their antioxidant activity. In conclusion, 734THIF nanoparticles are characterized by improved physicochemical properties, increased water solubility, and enhanced skin penetration, and these may have potential use in the future as a topical delivery formulation for the treatment of skin diseases.

Keywords: 7,3′,4′-trihydroxyisoflavone, nanoparticles, water solubility, skin penetration, topical delivery

Introduction

Soybean products, such as soybean milk, miso, and tofu, are popular foods in Asian countries and worldwide. A number of epidemiological studies have indicated that soybean products are effective in preventing the progression of diseases, including diabetes,[1] menopause syndrome,[2] cardiovascular disease,[3] cancer,[4] and viral infections.[5] The main active compounds in soybean products are daidzein and genistein, which are generally recognized as phytoestrogens.[6] Previous studies have also demonstrated that these isoflavones possess many pharmacological activities

such as anticancer,[7] antioxidant,[8] anti-inflammation,[9] and photoprotective effects.[10] 7,3′,4′-Trihydroxyisoflavone (734THIF; Figure 1) is a secondary metabolite of genistein,[11] and has been recently found to possess antioxidant,[12] melanin inhibition,[13] and skin cancer chemopreventive activities.[14] It is well known that the poor water solubility of genistein hinders its absorption and skin penetration and, therefore, limits its pharmacological effects when applied topically to the skin.[15,16] Similarly, 734THIF has a similar chemical backbone structure with poor water solubility, which limits its application in medicine and the cosmeceutical and food industry.

Over the past decade, drug delivery systems, including liposomes,[17] nanoparticles,[18] microemulsions,[19] and cyclo-dextrin inclusion complexes, have been used to overcome the poor water solubility and enhance the skin penetration and biological activity of the active ingredients.[20] Polymeric nanoparticle preparation is a form of nanoparticle engineering, which effectively decreases particle size and increases the surface area, thereby enhancing the solubility and penetration of active ingredients into deeper skin layers.[21] Previous studies have also demonstrated that eudragit acid-responsive polymer series are promising nanocarriers for efficient active ingredients delivery and may improve the clinical use of agents such as adapalene,[22] heparin,[23] and naproxen.[24] However, the improvements of solubility, skin penetration, and cell safety of 734THIF nanoparticle preparation have not yet been investigated.

The purpose of this study was to use the nanoprecipitation method to prepare optimal eudragit E100 (EE)–polyvinyl alcohol (PVA)-loaded 734THIF nanoparticles (734N) to improve its physicochemical properties and thereby increase its water solubility, skin penetration, and biological activities. This 734N delivery system was characterized by its particle size, morphology, encapsulation efficiency, drug loading efficiency, and water solubility. Moreover, the cell safety, in vitro skin penetration, and antioxidant activity of 734N were determined and compared with that of the raw 734THIF suspension.
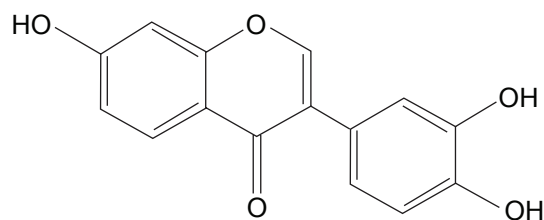

Figure 1 The chemical structure of 734THIF.
Abbreviation: 734THIF, 7,3′,4′-trihydroxyisoflavone.

Materials and methods
Materials
734THIF was obtained from Prof Chih-Hua Tseng (School of Pharmacy, College of Pharmacy, Kaohsiung Medical University, Kaohsiung, Taiwan). EE was a kind gift from Röhm Pharma (Darmstadt, Germany). PVA, 2,2-diphenyl-1-picrylhydrazyl (DPPH), and dimethyl sulfoxide (DMSO) were purchased from Sigma-Aldrich Chemicals Co. (St Louis, MO, USA). Dulbecco's Modified Eagle's Medium (DMEM), penicillin G, streptomycin, and amphotericin B were purchased from GIBCO BRL (Gaithersburg, MD, USA). HaCaT keratinocyte cell line was kindly provided by Professor Jeff Yi-Fu Chen (Department of Biotechnology, Kaohsiung Medical University, Kaohsiung, Taiwan). All other chemicals were of reagent grade, and all solvents were of high-performance liquid chromatography (HPLC) grade. Kaohsiung Medical University does not require institutional ethical approval for use of human cell lines.

Preparation of EE–PVA-loaded 734THIF nanoparticles (734N) and blank EE–PVA nanoparticles (blank-N)
This study used EE and PVA nanocarriers to encapsulate 734THIF by using the nanoprecipitation method.[25] As listed in Table 1, the organic phase consisted of various ratios of EE with 20 mg of 734THIF in 10 mL of ethanol, which was quickly injected into 40 mL of aqueous phase containing various ratios of PVA. During the injection process, the mixed solution was homogenized at 22,000 rpm for 5 minutes. Subsequently, ethanol in the mixed solution was immediately removed using a rotary vacuum evaporation system at 40°C. The remaining solution was filtered with filter paper (Advantec No 1, Toyo Roshi Kaisha, Tokyo, Japan) to obtain a stable nanoparticle delivery system (734N and blank-N). The 734N and blank-N were lyophilized with a freeze-dryer for 24 hours, and then the lyophilized powders were placed in a moisture-proof container until further experiments. All the nanoparticle preparations were performed in triplicate.

Table 1 Composition of 734THIF polymeric nanoparticle systems (734N) and blank EE–PVA nanoparticle (blank-N)

Ratio	734THIF (mg)	EE100/alcohol (mg/mL)	PVA/H$_2$O (mg/mL)
1:8:8	20	160/10	160/40
1:4:4	20	80/10	80/40
1:2:2	20	40/10	40/40
Blank-N	–	160/10	160/40

Abbreviations: 734THIF, 7,3′,4′-trihydroxyisoflavone; EE, eudragit E100; PVA, polyvinyl alcohol.

Morphology and particle size analysis

The mean particle size of 734N was determined using a Zetasizer 3000 HS analyzer (Malvern Instruments, Malvern, UK). The 734N solution was diluted tenfold with distilled water and placed in a cuvette for particle analysis. The experiments were performed in triplicate. In addition, the morphology of 734N was observed by transmission electron microscopy (TEM) analysis (JEM-2000EXII instrument, JEOL Co., Tokyo, Japan). 734N was diluted 50-fold in pure water, placed onto a carbon-coated copper grid, and immediately stained with 0.5% (w/v) phospho-tungstic acid. The sample was stored in a moisture-proof container until analysis. In addition, the shape and surface characteristics of lyophilized powder of 734THIF and 734N were observed using a scanning electron microscope (SEM; Hitachi S4700, Hitachi, Tokyo, Japan). Each sample was sputter-coated with gold–palladium under an argon atmosphere using a gold sputter module in a high-vacuum evaporator and then immediately determined using SEM set at 15 kV.

HPLC analysis of 734THIF

The HPLC analysis system (LaChrom Elite L-2000, Hitachi) consisted of an L-2130 pump, L-2200 autosampler, and L-2420 ultraviolet–visible (UV–vis) detector. The analysis was carried out using the Mightysil RP-18 GP column (250×4.6 mm id, 5 µm). The mobile phase consisted of acetonitrile and 10 mM KH_2PO_4 (35:65, v/v). The pH value was adjusted to 2.8 using phosphoric acid. The flow rate was set at 1.0 mL/min. The wavelength of the UV detector was set at 262 nm. The chromatogram of 734THIF is shown in Figure 2, showing that the retention time for 734THIF appeared at 4.8 minutes. The 734THIF concentration of all nanoparticle samples was determined using a linear calibration curve (r=0.999) of 734THIF within the range of 0.01–50 µg/mL.
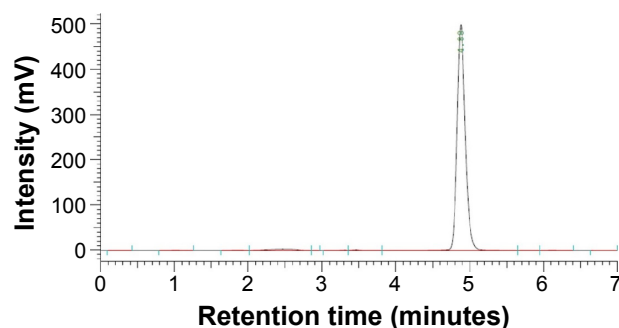

Figure 2 The HPLC chromatogram of 734THIF.
Abbreviations: HPLC, high-performance liquid chromatography; 734THIF, 7,3',4'-trihydroxyisoflavone.

Drug loading and encapsulation efficiency of 734N

The drug loading and encapsulation efficiencies are important indexes for evaluating a successful pharmaceutical formulation. For drug loading determination, 50 µL of each sample was added into 950 µL of methanol, and the 734THIF concentration was immediately measured by the aforementioned HPLC method. For the determination of encapsulation efficiency, 200 µL of the sample was aspirated and added into centrifugal filter devices (Microcon YM-10, Millipore, Billerica, MA, USA) and then centrifuged at 10,000 rpm for 10 minutes. The encapsulated part was retained in the upper tube, while the unencapsulated part was collected from the lower tube. The amount of unencapsulated 734THIF was detected by the aforementioned HPLC method. The drug loading and encapsulation efficiencies of 734N could be calculated by following equations:

$$\text{Drug loading (\%)} = \frac{C_{734THIF} \times V_{734N}}{W_{734THIF}} \times 100\% \quad (1)$$

$$\text{Encapsulation efficiency (\%)} = \frac{C_{734THIF}\, V_{734N} - C_{unentrapped}\, V_{734N}}{C_{734THIF}\, V_{734N}} \times 100\%, \quad (2)$$

where $C_{734THIF}$ is the concentration of 734THIF from 734N, $W_{734THIF}$ is the theoretical amount of 734THIF added, V_{734N} is the volume of 734N, and $C_{unentrapped}$ is the concentration of unencapsulated 734THIF.

In vitro solubility of 734THIF and 734N

In vitro solubility studies of 734THIF and its nanoparticle system were carried out in pH 3.5, pH 5.5, and pH 7.4 of 0.2 M KH_2PO_4 buffer solutions. One milligram of 734THIF and 734N were respectively added into 1 mL of various buffer solutions, and then agitated with a shaker at 5, 10, 30, 60, and 120 minutes. Subsequently, all samples were filtered with a 0.45 µm syringe filter. The concentration of 734THIF from each time point was determined by HPLC analysis.

Determination of hydrogen-bond formation of 734THIF and 734N

The spectra of [1]H-nuclear magnetic resonance (^{1}H-NMR) analyses were used to evaluate hydrogen-bond formation between 734THIF and EE–PVA polymer. A Varian Mercury Plus 400 Actively Shielded NMR System (Oxford Instrument Co., Oxfordshire, UK) was used to record the ^{1}H-NMR spectra of raw 734THIF, 734N, and blank-N. Briefly, 2 mg of

each sample was dissolved in 0.8 mL of DMSO-d_6 and then placed into the NMR system to obtain the ^{1}H-NMR spectra. In addition, Fourier transform infrared (FTIR) spectra were determined using a Perkin-Elmer 2000 spectrophotometer (Perkin-Elmer, Norwalk, CT, USA). Each sample was mixed with potassium bromide (KBr) evenly by a mortar and compressed into a thin tablet for analysis. The scanning range was set at 400–4,000 cm^{-1}.

Determination of crystalline-to-amorphous transformation of 734THIF and 734N

The crystalline form of 734THIF, 734N, and blank-N was determined by powder X-ray diffractometry (XRD) analysis using a Siemens D5000 instrument (Siemens, Munich, Germany) with Cu–Kα radiation at 40 kV and 80 mA. The scanning angle (2θ) was set from 2° to 50°, with the scanning rate at 1°/min. In addition, we also used differential scanning calorimetry (DSC) to confirm the crystalline-to-amorphous transformation of each sample. In brief, approximately 3 mg of 734THIF, 734N, and blank-N were placed into separate aluminum pans and then put into the differential thermal analyzer (Perkin-Elmer). The temperature for scanning was set at 200°C, the scanning rate was 10°C/min, and the final temperature was 320°C.

In vitro skin penetration of 734THIF and 734N

This experiment was performed using the European Cosmetic Toiletry and Perfumery Association (COLIPA) guideline standard protocol.[26] In brief, fresh pig skin from the flank region was obtained from a local butcher and cut into appropriate sizes and mounted carefully on Franz diffusion cells. The stratum corneum faced the donor chamber and the dermis side was placed on the receptor chamber. The receptor fluid (containing 0.14 M NaCl, 2 mM K_2HPO_4, 0.4 mM KH_2PO_4, 10% Penicillin, pH 7.4) was added into the receptor chamber. The Franz diffusion cells were maintained at 32°C and stirred at 600 rpm throughout the experiment. At the start, 200 μL of each sample (n=5) was topically applied onto the donor side at different time points (1, 2, 4, and 8 hours). After termination of the experiment, the residual test sample was removed from the skin by aspiration, and the stratum corneum of each sample was obtained by 15 times of tape-stripping. The epidermis and dermis layers were cut into small pieces, and then all samples were immersed in 2 mL of methanol and placed in a sonicated water bath for 1 hour to extract 734THIF from the skin. The content of 734THIF in each sample was determined by HPLC method.

Cell safety assay of 734N

HaCaT keratinocytes were cultured in DMEM medium (GIBCO) containing 10% fetal bovine serum (Hazelton Product, Denver, PA, USA) and 1% penicillin–streptomycin at 37°C in 5% CO_2. When the cultures reached confluence, cells were treated with 0.05% (w/v) trypsin/0.53 mM ethylenediaminetetraacetic acid (EDTA) for 5 minutes at 37°C. The cell toxicity and changes from normal morphology were evaluated using the "Qualitative morphological grading of cytotoxicity of extracts" from ISO 10993-Part 5. In brief, 1×10^4 HaCaT keratinocytes in 100 μL of culture medium were seeded in 96-well plates and allowed to adhere for 24 hours. After incubation, the cell culture medium was removed and cells were treated with different concentrations of each sample in treatment medium. After 24 hours of treatment, 150 μL of MTT solution was added to each well and then incubated for 4 hours at 37°C. After incubation, the absorbance of the plate was measured at 550 nm using a microplate spectrophotometer (BioTek μQuant, Winooski, VT, USA). Each experiment was performed three times, and cell viability was calculated by the following formula:

$$\text{Cell viability (\%)} = \frac{\text{OD}_{550} \text{of test sample}}{\text{OD}_{550} \text{of blank}} \times 100\% \quad (3)$$

DPPH scavenging activity

The DPPH scavenging ability was evaluated according to a modified method from Yen et al.[27] 734THIF was dissolved in DMSO (734D) and distilled water (734H) at different concentrations, and 734N was also prepared at multiple concentrations. Subsequently, 100 μL of 200 μM DPPH was mixed with 100 μL of each sample and incubated in a dark room for 30 minutes. The absorbance of the reaction solution was determined using a microplate spectrophotometer (μQuant, Biotek Instruments) at 517 nm. The DPPH scavenging ability was evaluated using the following equation: Scavenging effect (%) = [(control − sample)/control] ×100%. The concentration of each sample reaching 50% of scavenging activity (SC_{50}) was used to compare the antioxidant ability of each sample.

Statistical analysis

All data were expressed as mean ± standard deviation. Statistical analysis was performed with one-way analysis of variance test using SPSS 13.0 software (SPSS Inc., Chicago, IL, USA). P-value <0.05 was considered to be statistically significant.

Results and discussion

This is the first study to successfully prepare an optimal EE–PVA polymer-loaded 734THIF nanoparticle system (734N) using the nanoprecipitation method. Our results demonstrated that an optimal nanoparticle delivery formulation can improve the physicochemical properties of raw 734THIF, including particle size nanonization, good encapsulation efficiency, hydrogen-bond formation, and amorphous transformation. This resulted in an enhancement of water solubility, cellular uptake, and in vitro skin penetration. In addition, 734THIF is a good antioxidant, but its activity is decayed by light and heat. Our data indicated that 734N maintained the free radical scavenging effect, thus showing that nanoprecipitation is a suitable nanoparticle engineering process for 734THIF.

Optimal nanoparticle delivery formulation of 734THIF

It is well known that nanoparticle preparation is a good method to improve the physicochemical properties of active hydrophobic compounds such as quercetin,[28] genistein,[29] and curcumin.[30] As listed in Table 1, this study used different ratios of raw 734THIF, EE, and PVA to prepare an optimal 734N formulation. As shown in Table 2 and Figure 3A–D, raw 734THIF had size in the micrometer range (4,849.33±256.86 nm) and a polydispersity index (PI) higher than 1, which indicated that the particle size of 734THIF had a broad distribution. The lower ratio formulation of 734THIF:EE:PVA, 1:2:2 and 1:4:4, had size in the nanometer range (167.20±24.87, 106.73±3.21 nm, respectively), but PI was found to be ~0.8, which indicated that the particle size of the sample still had a broad distribution. When the polymer ratio increased (734THIF:EE:PVA, 1:8:8), the particle size and PI value of 734N were 57.53±2.49 nm and 0.45, respectively. These results indicated that the mean particle size and narrow size distribution of 734N are dependent on the ratio of EE and PVA. In addition, this study also observed the morphology of 734N, and the TEM images indicated that 734N displayed a smaller nanocapsule structure and more uniform size distribution, with particle sizes

<100 nm (Figure 3E). A possible explanation is that a high ratio of EE and PVA could reduce their particle size and size distribution, resulting in sufficient stabilization of the 734N nanoparticles system.

Previously, Mora-Huertas et al[31] indicated that the drug loading and encapsulation efficiencies are the major factors affecting the success of nanoparticle formulations on drug absorption and release. Our data indicated that the lower ratio formulation of 734THIF:EE:PVA (1:2:2 and 1:4:4) had 734THIF drug loading efficiency of <60% (51.57% and 57.23%, respectively), while the higher ratio formulation (1:8:8) had 734THIF drug loading efficiency of 83.45%. In addition, the encapsulation efficiency of 734THIF was dependent on the ratio of EE and PVA, and the higher ratio 734N system (734THIF:EE:PVA at 1:8:8) showed encapsulation efficiency >98% (Table 2). The possible reason is that the nanoprecipitation method used two phases for preparing the nanoparticle system, namely, the organic and aqueous phases. The higher ratio of EE allowed 734THIF to be preferentially dispersed in the organic phase, which was then added into the PVA aqueous phase to form a stable EE–PVA–734THIF system. Previous studies have also demonstrated that PVA is an effective emulsion stabilizer used to stabilize nanoparticle systems.[32,33] The hydrophilic and hydrophobic portion of PVA can interpenetrate into EE–734THIF during the nanoprecipitation process and remain trapped in the polymeric matrix of the nanoparticles, resulting in a stable nanoparticle delivery system, thus enhancing the encapsulation efficiencies of 734THIF. Consequently, 734N system (734THIF:EE:PVA at 1:8:8) is the optimal nanoparticle formulation.

The correlation between physicochemical properties and optimal 734N formulation

On the basis of our knowledge, the improvement of physicochemical properties, including reduction of particle size, amorphous transformations, and intermolecular hydrogen-bond formation, can effectively increase the drug loading and encapsulation efficiencies of active ingredients and further enhance their drug absorption, penetration,

Table 2 The drug loading efficiency, encapsulation efficiency, particle size, and PI of 734THIF polymeric nanoparticle systems

Ratio	Drug loading (%)	Encapsulation efficiency (%)	Particle size (nm)	PI
1:8:8	83.45±2.33	98.10±0.84	57.53±2.49*	0.45±0.01*
1:4:4	57.23±7.37	94.05±1.06	106.73±3.21*	0.80±0.11
1:2:2	51.57±1.73	88.50±1.77	167.20±24.87*	0.83±0.12
734THIF			4,849.33±256.86	>1.0

Notes: Values are mean ± SD (n=3). *$P<0.05$: statistically significant difference compared with 734THIF.
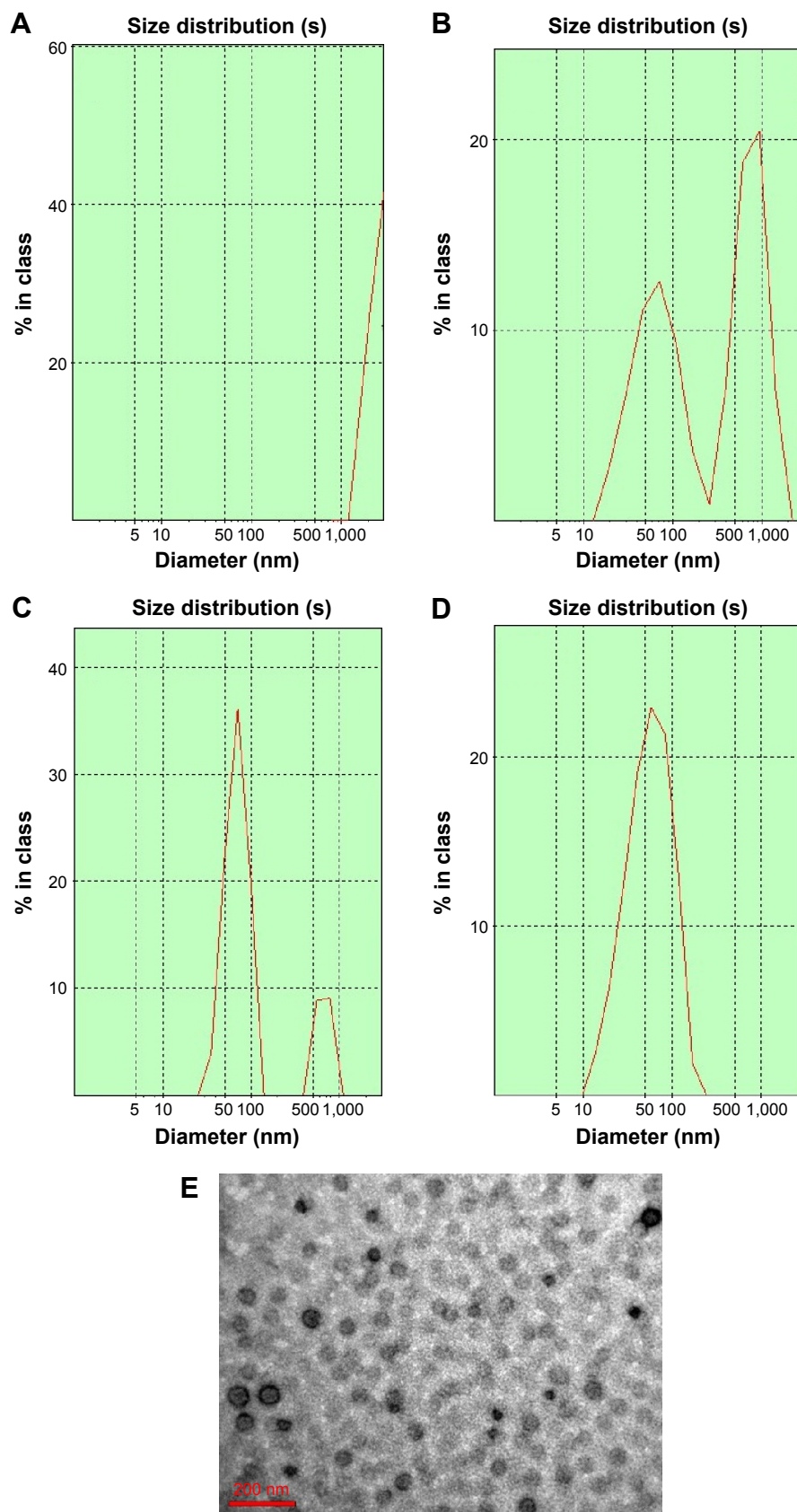**Abbreviations:** 734THIF, 7,3′,4′-trihydroxyisoflavone; PI, polydispersity index; SD, standard deviation.

A Size distribution (s)

B Size distribution (s)

C Size distribution (s)

D Size distribution (s)

E

Figure 3 Particle size distribution and morphology of 734THIF nanoparticle formulations.
Notes: Particle size distribution of (**A**) raw 734THIF, (**B**) 734THIF:EE:PVA (1:2:2), (**C**) 734THIF:EE:PVA (1:4:4), (**D**) 734THIF:EE:PVA (1:8:8). (**E**) Morphology of 734THIF:EE:PVA (1:8:8) by TEM.
Abbreviations: 734THIF, 7,3′,4′-trihydroxyisoflavone; PVA, polyvinyl alcohol; EE, eudragit E100; TEM, transmission electron microscopy; 734N, 734THIF nanoparticles.

and release.[34] DSC and XRD are usually used to elucidate the crystal-to-amorphous transformations for nanoparticle systems, such as curcumin[27] and genistein,[29] and were therefore applied in this study. Powder XRD patterns of 734THIF, 734N, and blank-N are shown in Figure 4A. The characteristic peaks of raw 734THIF appeared at diffraction angles of 9.1°, 23.6°, 27.9°, and 36.7°, which indicate a highly crystalline structure. On the other hand, blank-N did not show any obvious peak, and all of the characteristic peaks disappeared in the XRD pattern of 734N, indicating that the crystal structure of 734THIF had indeed transformed into an amorphous state in 734N. In addition, Figure 4B shows the DSC thermograms of raw 734THIF, 734N, and blank-N. An obvious endothermic melting peak for raw 734THIF was observed at 293.3°C, which also indicated the crystalline form of raw 734THIF. Blank-N exhibited no endothermic melting peak. After the nanoprecipitation process, the endothermic peak of raw 734THIF completely disappeared. According to these findings, we suggest that following nanoprecipitation, the raw 734THIF was dispersed throughout the EE–PVA polymers and then encapsulated within the matrix by forming a high-energy amorphous complex with intermolecular interactions. Some studies have also demonstrated that EE–PVA effectively changed the crystalline structure of hydrophobic compounds such as quercetin,[28] kaempferol,[35] and silybinin.[36]

In addition, we further investigated the intermolecular interactions of EE–PVA polymer with 734THIF using FTIR spectrometry and ^{1}H-NMR spectroscopy. FTIR spectra of raw 734THIF, 734N, and blank-N are shown in Figure 5A. The FTIR spectra of 734THIF demonstrated several characteristic peaks, including a broad band at 3,420–3,100 cm^{-1}, corresponding to the phenolic–OH group, aromatic C=C stretching band in the range of 1,600–1,400 cm^{-1}, carbonyl group (C=O) stretching vibration at 1,625 cm^{-1}, and C–O–H stretching band at 1,288 cm^{-1}. On the other hand, the FTIR spectra of 734N and blank-N demonstrated a C=O ester stretch peak at 1,729 and 1,735 cm^{-1} and polymer CH stretch at 2,947 cm^{-1}, respectively. In the FTIR spectra of 734N, phenolic–OH stretch of 734THIF became a broader band and entirely disappeared at 3,391 cm^{-1}. This implies hydrogen bonding of the hydroxyl groups of 734THIF with the EE–PVA polymer. Furthermore, the ^{1}H-NMR spectrum of 734THIF indicated that the resonance peaks for aromatic protons and phenolic protons were found in the regions of δ6.7–8.3 and δ8.9–10.8, respectively. After nanoprecipitation process, the clear signal of phenolic protons on 734THIF, δ10.798 (C7–OH), δ9.029 (C4′–OH), and δ8.981 (C3′–OH) disappeared in the ^{1}H-NMR spectrum of 734N (Figure 5B). These results indicated that the phenolic–OH on A and B rings of 734THIF effectively formed an intermolecular hydrogen bond with EE–PVA polymer. The occurrence of intermolecular hydrogen bonding probably contributes to better water solubility of 734N, and similar results had been found in quercetin[28] and kaempferol.[35] Therefore, EE–PVA functions as a suitable polymer to encapsulate 734THIF to form a stable nanoparticle system during the nanoprecipitation process.

Optimal 734N exhibited increased water solubility and skin penetration without cell toxicity

Since most of the active ingredients do not have the ability to penetrate the natural skin barrier (stratum corneum), skin
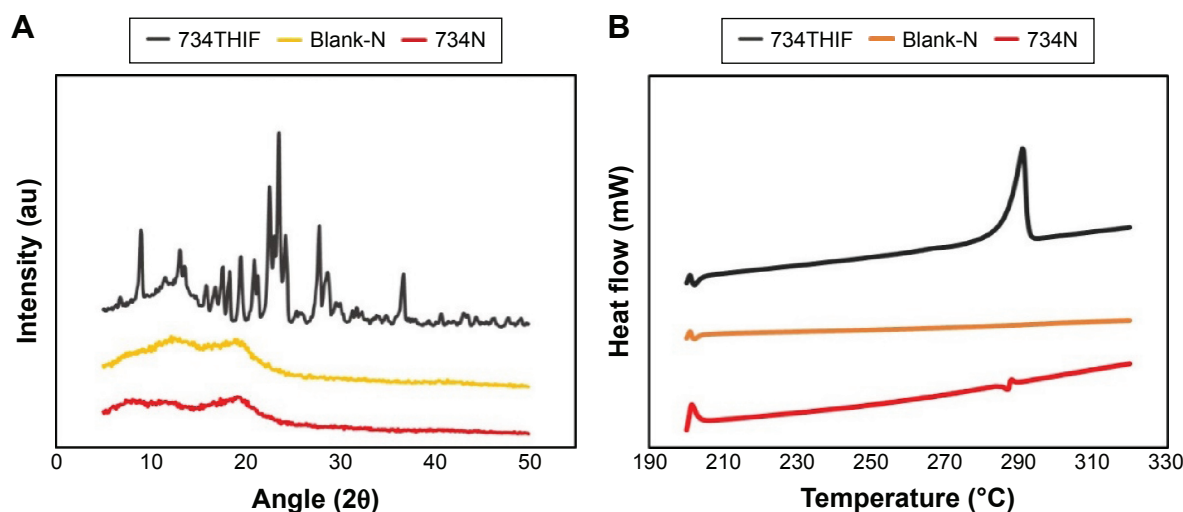

Figure 4 Crystalline-to-amorphous transformation of 734THIF nanoparticle formulation, as demonstrated by (**A**) powder XRD and (**B**) DSC.
Abbreviations: 734THIF, 7,3′,4′-trihydroxyisoflavone; XRD, X-ray diffractometry; DSC, differential scanning calorimetry.
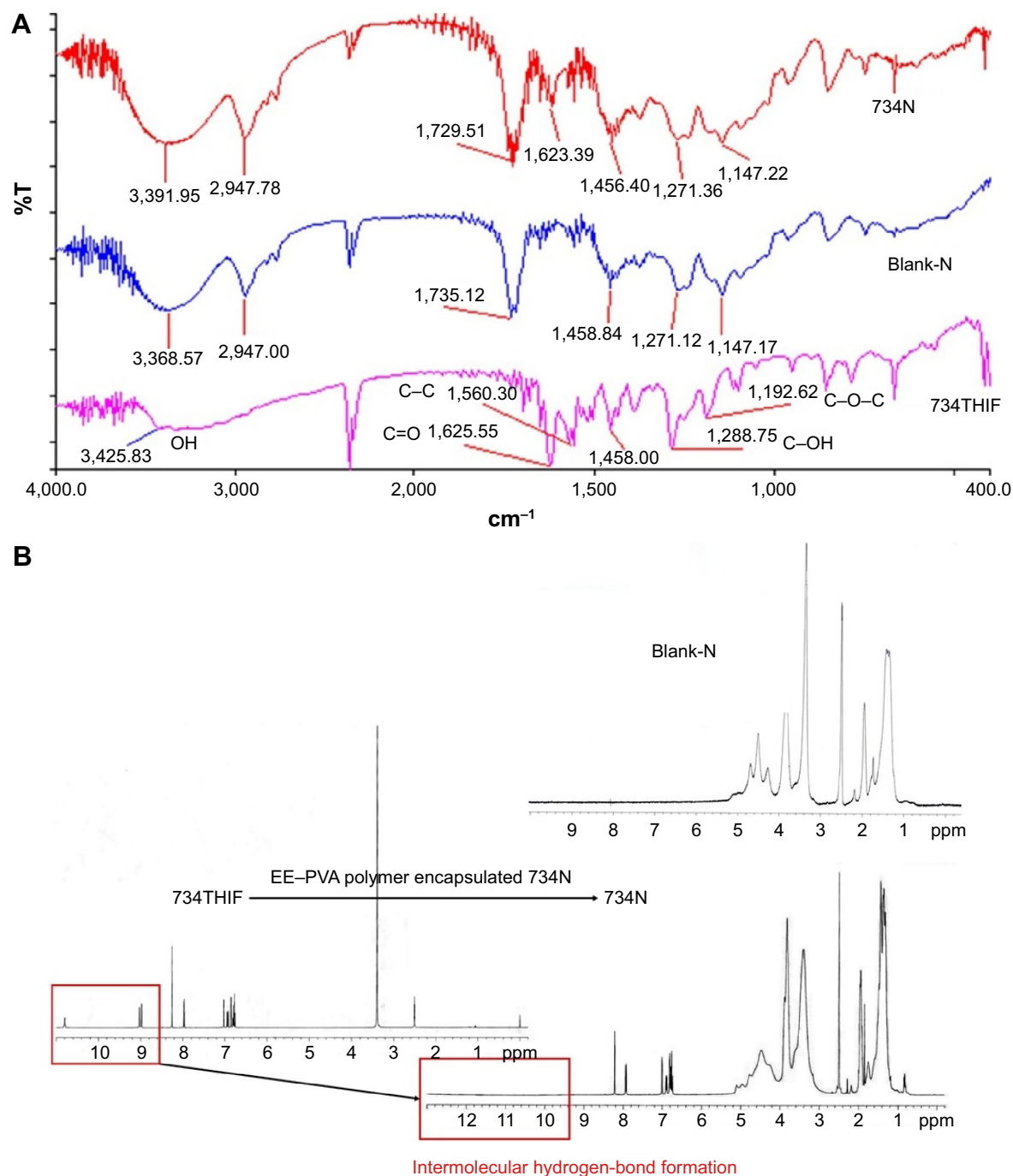
Figure 5 Intermolecular hydrogen-bond formation between EE–PVA polymer and 734THIF, as demonstrated by (**A**) FTIR and (**B**) ¹H-NMR spectra.
Abbreviations: 734THIF, 7,3′,4′-trihydroxyisoflavone; EE, eudragit E100; PVA, polyvinyl alcohol; FTIR, Fourier transform infrared; ¹H-NMR, ¹H-nuclear magnetic resonance; ppm, parts per million.

penetration enhancers have been developed to enhance their water solubility and skin penetration to help deliver them into the deeper skin layers. According to the Generally Recognized as Safe guidelines of the US Food and Drug Administration, the ideal skin penetration enhancer should possess several advantages, including having reversible action on skin and being pharmacologically inert, nontoxic, nonirritating, and nonallergenic.[37] Polymers are one of the commonly used potential enhancers (eg, eudragit, chitosan, and PVA), and polymer-based nanoparticles can enhance the water solubility and skin penetration of active ingredients in medicine and cosmetic industries.[31] This the first study to use EE–PVA as a skin penetration enhancer to prepare polymer-based nanoparticles of 734THIF, and we further

determined its cell safety using in vitro cytotoxicity assay. The cell viability of 734N using MTT assay is shown in Figure 6A, showing that different concentrations of 734N did not exhibit any obvious cell toxicity when compared with 1% DMSO treatment in HaCaT keratinocytes. The cell morphologies following 734N treatment did not display cytotoxic features such as changes in general morphology, vacuolization, detachment, cell lysis, and membrane integrity (data not shown). These results indicated that EE–PVA-loaded 734THIF did not exhibit in vitro cytotoxicity, and therefore 734N is a safe polymer-based nanoparticle formulation.

Furthermore, Lane[38] indicated that the drug solubility in the skin penetration enhancer has an important effect on ultimate drug concentration in the skin in vivo, and defined this finding as "Diffusion-Partition-Solubility theory". The photographs of 734N in solutions with different pH values are shown in Figure 6B. 734N redispersed in pH 3.5 and pH 5.5 buffer solutions present as clear solutions. However, a

suspension was seen when 734N was redispersed in pH 7.4 buffer solution. This study is the first to report the water solubility of 734THIF in different pH values of phosphate buffer solution at various times. The 734THIF water solubility in pH 3.5 (lower accepted value in cosmetic) and pH 5.5 (suitable value in skin) after 120 minutes of agitation was <20 μg/mL, and in pH 7.4 (suitable value in blood) was ~40 μg/mL (Figure 6C). In contrast, the water solubility of 734N in pH 3.5, pH 5.5, and pH 7.4 after 120 minutes of agitation was 778, 753, and 73 μg/mL, respectively (Figure 6D). These results indicated that the EE–PVA polymer system effectively encapsulated 734THIF into a nanoparticle system and also overcame the poor water solubility of 734THIF. The possible reason for water solubility improvement is that the EE, an acid-responsive polymer with ionization of amino groups, quickly solubilized in the lower pH water solutions (pH 3.5 and pH 5.5) and exhibited a fast drug release due to the stability of the 734THIF nanoparticle solution. However, the higher pH solution (pH 7.4) did not allow 734N to
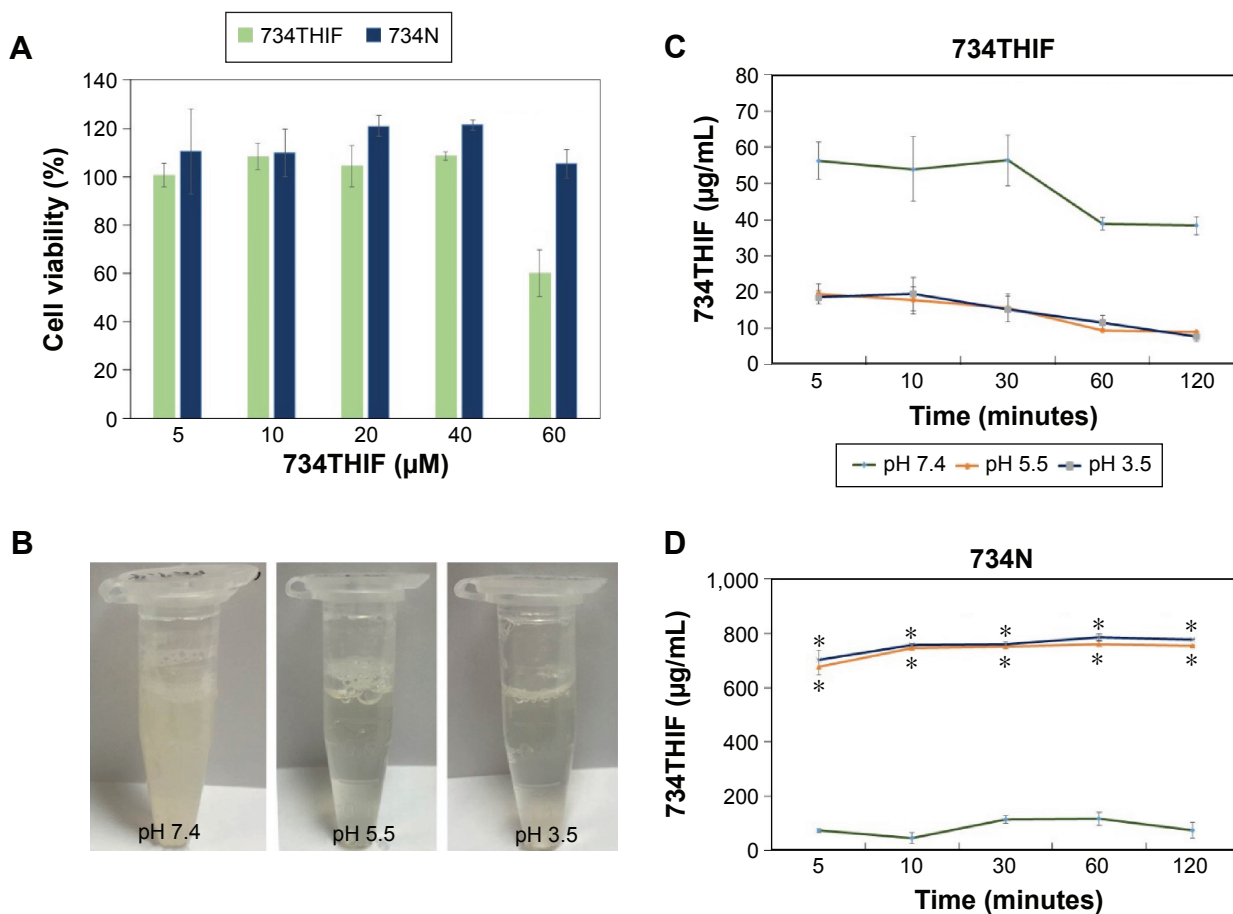

Figure 6 (**A**) The cell viability of 734THIF nanoparticle formulation. (**B**) Photographs of 734N dispersed in various pH buffer solutions. The solubility of 734THIF (**C**) and 734N (**D**) in 0.2 M KH_2PO_4 buffer solution at various pH.
Note: *$P < 0.05$ was statistically significant difference compared with 734THIF.
Abbreviations: 734THIF, 7,3′,4′-trihydroxyisoflavone; 734N, 734THIF nanoparticles.

disperse as a nanoparticle solution and resulted in poor water solubility, as seen in Figure 6D.

In addition, we also used SEM to observe the morphology of raw 734THIF and 734N to elucidate their surface characteristics (Figure 7). Irregular powder ranging in size from 10 to 30 μm was found in raw 734THIF, while 734N was characterized by an obvious regular rectangular slice form. These results indicated that 734N had higher surface area than raw 734THIF and might exhibit good water solubility.

Moreover, we further performed in vitro skin penetration assay to compare the skin penetration of raw 734THIF and 734N at various times. The contents of 734THIF delivered from raw 734THIF and 734N to different skin layers are shown in Figure 8. When raw 734THIF solution was topically administered, the content of 734THIF retained in all skin layers was similar and not >7 μg/cm^2 at 1–8 hours, which indicated that raw 734THIF solution did not penetrate the skin in a time-dependent manner. Conversely, the content of 734THIF in 734N formulation that penetrated through all skin layers increased with time and was higher than raw 734THIF. When 734N was topically administered, a stable content of 734THIF was retained in the stratum corneum at various times and was 4.71-fold higher than raw 734THIF solution. In addition, 734N administration showed a significant enhancement in 734THIF penetration into the epidermal layer (from 13.81±2.22 to 19.54±3.37 μg/cm^2) and dermal layer (from 5.14±1.10 to 14.98±2.87 μg/cm^2). In other words, the total retained content of 734THIF from 734N penetrating through the epidermal and dermal layers was >5.05 times higher than raw 734THIF solution at 8 hours. According to these results, 734N had better hydration effect within the stratum corneum than raw 734THIF, and it also rapidly penetrated into the epidermis and dermis when compared to raw 734THIF.

Previously, Alvarez-Román et al[39] indicated that nanoparticles between 20 and 200 nm in size could accumulate in skin "furrows" and possess more opportunities for tight contact with the skin, resulting in more active ingredients being able to penetrate the stratum corneum and deeper skin layers. Our data demonstrated that EE–PVA polymer effectively nanonized the particle size of 734THIF (57.53±2.49 nm), helped in quick penetration of the stratum corneum, and allowed higher 734THIF content to be retained in epidermal and dermal layers. Furthermore, previous studies reported that topical nanoparticle delivery formulation could reduce the particle size of the active ingredient and increase its particle number to form a dense film, which results in an occlusion effect with increased skin hydration, and enhance the skin penetration of the active ingredient.[40–42] EE–PVA polymer has a plastic film property that can effectively encapsulate the 734THIF into a film-like nanoparticle formulation, leading to an occlusion effect on the skin surface, improvement in stratum corneum hydration, and enhanced penetration of 734THIF when compared to raw 734THIF solution. Collectively, we suggest that EE–PVA-loaded 734THIF nanoparticles can increase the water solubility of raw 734THIF and then enhance its skin penetration ability through improvement in physicochemical properties.

Determination of 734N free radical scavenging effect

734THIF, one of the secondary metabolites of daidzein and genistein, has a similar chemical structure to isoflavone in soybean food and possesses many pharmacological activities, including melanin inhibition, photoprotection,
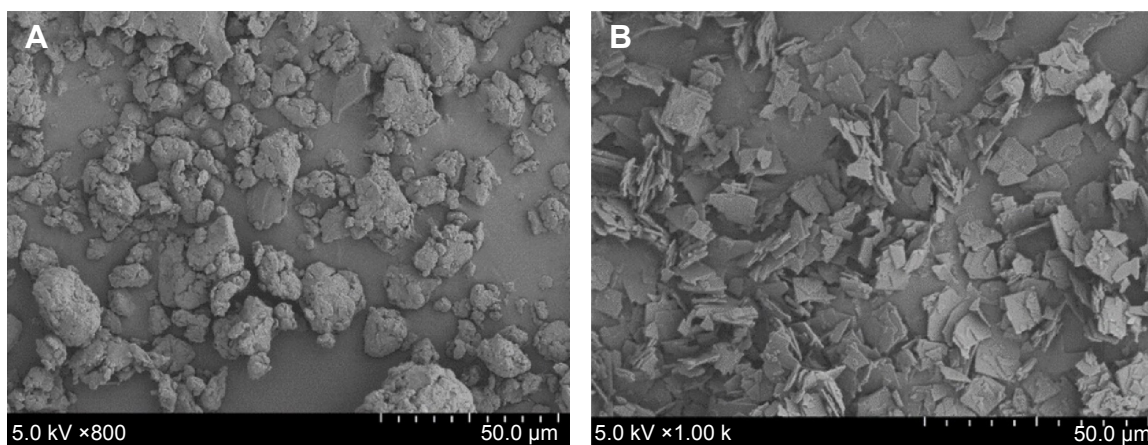

Figure 7 The surface morphology of lyophilized powder 734THIF (**A**) and 734THIF nanoparticle formulation (**B**), as shown by SEM.
Abbreviations: 734THIF, 7,3′,4′-trihydroxyisoflavone; SEM, scanning electron microscopy.
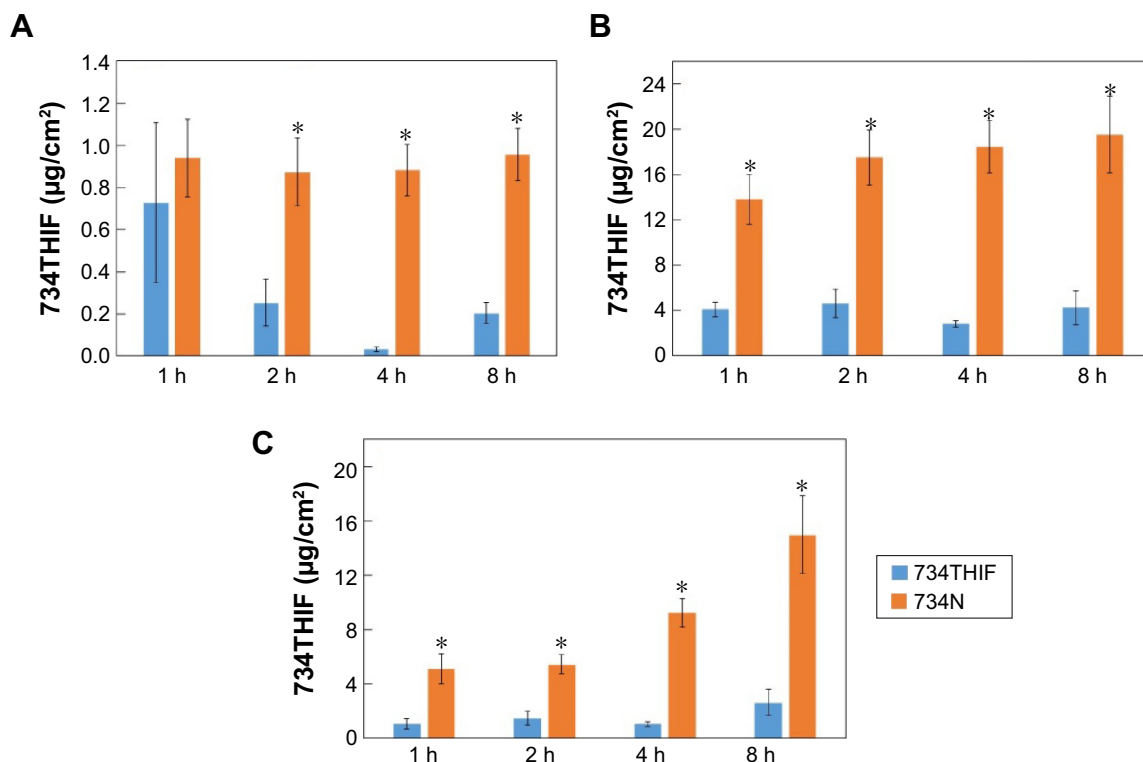
Figure 8 The contents of 734THIF delivered from raw 734THIF and 734N to different skin layers: stratum corneum (**A**), epidermis (**B**), and dermis (**C**).
Notes: Values are mean ± SD (n=5). *$P<0.05$: statistically significant difference compared with raw 734THIF.
Abbreviations: 734THIF, 7,3′,4′-trihydroxyisoflavone; h, hours; SD, standard deviation; 734N, 734THIF nanoparticles.

and antioxidant activity. Rostagno et al[43] reported that the stability of isoflavones is influenced by several factors, including processing temperature, duration of heating, photosensitization under light exposure, pH, and the presence of microorganisms. Our study used a nanoprecipitation method to prepare 734N formulation using high-speed homogenization, and these processes easily generated higher processing temperatures and exposure to light. These conditions may lead to degradation of isoflavone and influence its pharmacological activities. Because of these factors, we performed the DPPH free radical scavenging assay to validate the antioxidant activities of 734N. Figure 9 shows that 734THIF in DMSO and 734N in water were effective in scavenging DPPH free radicals in a dose-dependent manner. The SC_{50} value (concentration of sample required to scavenge 50% of DPPH free radicals) of 734THIF in DMSO and 734N in water was 12.09±1.65 and 14.77±0.58 µg/mL, respectively, and there was no statistically significant difference between them (Table 3). However, 734THIF in water at the same concentrations did not exhibit obvious DPPH free radical scavenging effect. These results demonstrated that the nanoprecipitation process did not affect the DPPH free radical scavenging ability of 734THIF.

Conclusion

This study demonstrated that EE–PVA polymer-loaded 734THIF effectively increased the poor water solubility and led to better skin penetration than raw 734THIF solution
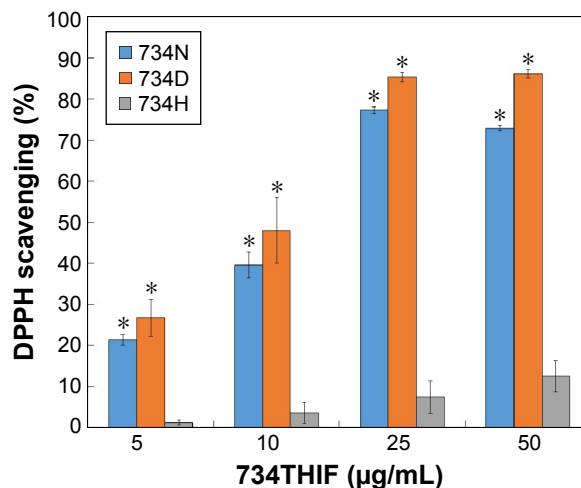

Figure 9 The DPPH radical scavenging activity of raw 734THIF suspended in deionized water (734H) and DMSO (734D), and 734THIF nanoparticle formulation suspended in deionized water (734N).
Notes: Values are mean ± SD (n=3). *$P<0.05$: statistically significant difference compared with 734H.
Abbreviations: DPPH, 2,2-diphenyl-1-picrylhydrazyl; 734THIF, 7,3′,4′-trihydroxyisoflavone; DMSO, dimethyl sulfoxide; SD, standard deviation.

Table 3 The concentration of raw 734THIF and 734 nanoparticle formulation required to scavenge 50% of DPPH free radicals (SC_{50})

Sample	SC_{50} (µg/mL)
734THIF in H_2O (734H)	NE
734THIF in DMSO (734D)	12.09±1.65
734THIF nanoparticles in H_2O	14.77±0.58

Notes: Values are mean ± SD (n=3).
Abbreviations: 734THIF, 7,3′,4′-trihydroxyisoflavone; DPPH, 2,2-diphenyl-1-picrylhydrazyl; SC_{50}, 50% of scavenging activity; DMSO, dimethyl sulfoxide; NE, no effect; SD, standard deviation.

by improving the physicochemical properties of 734THIF, including particle size reduction, amorphous transformation, and intermolecular hydrogen-bond formation with EE–PVA polymer. Furthermore, the 734THIF nanoparticle formulation showed better antioxidant activity than 734THIF solution, and it is also a safe formulation based on the results of the in vitro cytotoxicity study. Therefore, we suggest that EE–PVA polymer-loaded 734THIF could be a potential topical delivery formulation in pharmaceutical and cosmeceutical products for the management of various skin conditions.

Acknowledgments

Disclosure

The authors report no conflicts of interest in this work.

References

1. Moghaddam AS, Entezari MH, Iraj B, Askari GR, Maracy MR. The effects of consumption of bread fortified with soy bean flour on metabolic profile in type 2 diabetic women: a cross-over randomized controlled clinical trial. *Int J Prev Med*. 2014;5:1529–1536.
2. Acharjee S, Zhou JR, Elajami TK, Welty FK. Effect of soy nuts and equol status on blood pressure, lipids and inflammation in postmenopausal women stratified by metabolic syndrome status. *Metabolism*. 2015;64: 236–243.
3. Morimoto Y, Maskarinec G, Park SY, et al. Dietary isoflavone intake is not statistically significantly associated with breast cancer risk in the Multiethnic Cohort. *Br J Nutr*. 2014;112:976–983.
4. Talaei M, Koh WP, van Dam RM, Yuan JM, Pan A. Dietary soy intake is not associated with risk of cardiovascular disease mortality in Singapore Chinese adults. *J Nutr*. 2014;144:921–928.
5. Zhou J, Tzanetakis IE. Epidemiology of soybean vein necrosis-associated virus. *Phytopathology*. 2013;103:966–971.
6. Rusin A, Krawczyk Z, Grynkiewicz G, Gogler A, Zawisza-Puchałka J, Szeja W. Synthetic derivatives of genistein, their properties and possible applications. *Acta Biochim Pol*. 2010;57:23–34.
7. Mahmoud AM, Yang W, Bosland MC. Soy isoflavones and prostate cancer: a review of molecular mechanisms. *J Steroid Biochem Mol Biol*. 2014;140:116–132.
8. Mann GE, Rowlands DJ, Li FY, de Winter P, Siow RC. Activation of endothelial nitric oxide synthase by dietary isoflavones: role of NO in Nrf2-mediated antioxidant gene expression. *Cardiovasc Res*. 2007;75: 261–274.
9. Siriwardhana N, Kalupahana NS, Cekanova M, LeMieux M, Greer B, Moustaid-Moussa N. Modulation of adipose tissue inflammation by bioactive food compounds. *J Nutr Biochem*. 2013;24:613–623.
10. Lin JY, Tournas JA, Burch JA, Monteiro-Riviere NA, Zielinski J. Topical isoflavones provide effective photoprotection to skin. *Photodermatol Photoimmunol Photomed*. 2008;24:61–66.
11. Murata M, Midorikawa K, Koh M, Umezawa K, Kawanishi S. Genistein and daidzein induce cell proliferation and their metabolites cause oxidative DNA damage in relation to isoflavone-induced cancer of estrogen-sensitive organs. *Biochemistry*. 2004;43:2569–2577.
12. Park JS, Park HY, Kim DH, Kim DH, Kim HK. Ortho-Dihydroxyisoflavone derivatives from aged Doenjang (Korean fermented soypaste) and its radical scavenging activity. *Bioorg Med Chem Lett*. 2008; 18: 5006–5009.
13. Park JS, Kim DH, Lee JK, et al. Natural ortho-dihydroxyisoflavone derivatives from aged Korean fermented soybean paste as potent tyrosinase and melanin formation inhibitors. *Bioorg Med Chem Lett*. 2010; 20:1162–1164.
14. Lee DE, Lee KW, Byun S, et al. 7,3′,4′-Trihydroxyisoflavone, a metabolite of the soy isoflavone daidzein, suppresses ultraviolet B-induced skin cancer by targeting Cot and MKK4. *J Biol Chem*. 2011;286: 14246–14256.
15. Vitale DC, Piazza C, Melilli B, Drago F, Salomone S. Isoflavones: estrogenic activity, biological effect and bioavailability. *Eur J Drug Metab Pharmacokinet*. 2013;38:15–25.
16. Tang J, Xu N, Ji H, Liu H, Wang Z, Wu L. Eudragit nanoparticles containing genistein: formulation, development, and bioavailability assessment. *Int J Nanomedicine*. 2011;6:2429–2435.
17. Rahimpour Y, Hamishehkar H. Liposomes in cosmeceutics. *Expert Opin Drug Deliv*. 2012;9:443–455.
18. Papakostas D, Rancan F, Sterry W, Blume-Peytavi U, Vogt A. Nanoparticles in dermatology. *Arch Dermatol Res*. 2011;303:533–550.
19. Kreilgaard M. Influence of microemulsions on cutaneous drug delivery. *Adv Drug Deliv Rev*. 2002;54:S77–S98.
20. Aljuffali IA, Hsu CY, Lin YK, Fang JY. Cutaneous delivery of natural antioxidants: the enhancement approaches. *Curr Pharm Des*. 2015;21: 2745–2757.
21. Guterres SS, Alves MP, Pohlmann AR. Polymeric nanoparticles, nanospheres and nanocapsules, for cutaneous applications. *Drug Target Insights*. 2007;2:147–157.
22. Guo C, Khengar RH, Sun M, Wang Z, Fan A, Zhao Y. Acid-responsive polymeric nanocarriers for topical adapalene delivery. *Pharm Res*. 2014; 31:3051–3059.
23. Loira-Pastoriza C, Sapin-Minet A, Diab R, Grossiord JL, Maincent P. Low molecular weight heparin gels, based on nanoparticles, for topical delivery. *Int J Pharm*. 2012;426:256–262.
24. Ueda H, Wakabayashi S, Kikuchi J, Ida Y, Kadota K, Tozuka Y. Anomalous role change of tertiary amino and ester groups as hydrogen acceptors in eudragit E based solid dispersion depending on the concentration of naproxen. *Mol Pharm*. 2015;12:1050–1061.
25. Yen FL, Wu TH, Lin LT, Cham TM, Lin CC. Naringenin-loaded nanoparticles improve the physicochemical properties and the hepatoprotective effects of naringenin in orally-administered rats with CCl(4)-induced acute liver failure. *Pharm Res*. 2009;26:893–902.
26. COLIPA guidelines: Guidelines for Percutaneous Absorption/Penetration, 1997, Cosmetics Europe. Available from: http://www.jacvam.jp/files/doc/05_01/05_01_Z3.pdf. Accessed March 4, 2015.

27. Yen FL, Wu TH, Tzeng CW, Lin LT, Lin CC. Curcumin nanoparticles improve the physicochemical properties of curcumin and effectively enhance its antioxidant and antihepatoma activities. *J Agric Food Chem*. 2010;58:7376–7382.

28. Wu TH, Yen FL, Lin LT, Tsai TR, Lin CC, Cham TM. Preparation, physicochemical characterization, and antioxidant effects of quercetin nanoparticles. *Int J Pharm*. 2008;346:160–168.

29. Zhang W, Li X, Ye T, et al. Design, characterization, and in vitro cellular inhibition and uptake of optimized genistein-loaded NLC for the prevention of posterior capsular opacification using response surface methodology. *Int J Pharm*. 2013;454:354–366.

30. Naksuriya O, Okonogi S, Schiffelers RM, Hennink WE. Curcumin nanoformulations: a review of pharmaceutical properties and preclinical studies and clinical data related to cancer treatment. *Biomaterials*. 2014;35:3365–3383.

31. Mora-Huertas CE, Fessi H, Elaissari A. Polymer-based nanocapsules for drug delivery. *Int J Pharm*. 2010;385:113–142.

32. Sahoo SK, Panyam J, Prabha S, Labhasetwar V. Residual polyvinyl alcohol associated with poly(D,L-lactide-co-glycolide) nanoparticles affects their physical properties and cellular uptake. *J Control Release*. 2002;82:105–114.

33. Galindo-Rodriguez S, Allémann E, Fessi H, Doelker E. Physicochemical parameters associated with nanoparticle formation in the salting-out, emulsification–diffusion, and nanoprecipitation methods. *Pharm Res*. 2004;21:1428–1439.

34. Ernsting MJ, Murakami M, Roy A, Li SD. Factors controlling the pharmacokinetics, biodistribution and intratumoral penetration of nanoparticles. *J Control Release*. 2013;172:782–794.

35. Gohulkumar M, Gurushankar K, Rajendra Prasad N, Krishnakumar N. Enhanced cytotoxicity and apoptosis-induced anticancer effect of silibinin-loaded nanoparticles in oral carcinoma (KB) cells. *Mater Sci Eng C Mater Biol Appl*. 2014;41:274–282.

36. Tzeng CW, Yen FL, Wu TH, et al. Enhancement of dissolution and antioxidant activity of kaempferol using a nanoparticle engineering process. *J Agric Food Chem*. 2011;59:5073–5080.

37. Som I, Bhatia K, Yasir M. Status of surfactants as penetration enhancers in transdermal drug delivery. *J Pharm Bioallied Sci*. 2012;4:2–9.

38. Lane ME. Skin penetration enhancers. *Int J Pharm*. 2013;447:12–21.

39. Alvarez-Román R, Naik A, Kalia YN, Guy RH, Fessi H. Skin penetration and distribution of polymeric nanoparticles. *J Control Release*. 2004;99:53–62.

40. Müller RH, Petersen RD, Hommoss A, Pardeike J. Nanostructured lipid carriers (NLC) in cosmetic dermal products. *Adv Drug Deliv Rev*. 2007;59:522–530.

41. Loo Ch, Basri M, Ismail R, et al. Effect of compositions in nanostructured lipid carriers (NLC) on skin hydration and occlusion. *Int J Nanomedicine*. 2013;8:13–22.

42. Okonogi S, Riangjanapatee P. Physicochemical characterization of lycopene-loaded nanostructured lipid carrier formulations for topical administration. *Int J Pharm*. 2015;478:726–735.

43. Rostagno MA, Villares A, Guillamón E, García-Lafuente A, Martínez JA. Sample preparation for the analysis of isoflavones from soybeans and soy foods. *J Chromatogr A*. 2009;1216:2–29.